Check for updates

The FEBS Journal

FEBS PRESS science publishing by scientists

Hydrothermal origin of metabolic phosphorylation

Manon L. Schlikker[1], Nadja K. Hoffmann[1], Sabine Metzger[1,2], Jorge Moral-Pombo[3], Harun Tüysüz[3] and William F. Martin[1]

1 Institute of Molecular Evolution, Faculty of Mathematics and Natural Sciences, Heinrich Heine University Düsseldorf, Germany
2 Biocenter MS-Platform, University of Cologne, Germany
3 Catalysis and Energy Materials Group, IMDEA Materials Institute, Madrid, Spain

Keywords
bioenergetics; origin of life; origin of metabolism; phosphite; serpentinization

Correspondence
M. L. Schlikker, Institute of Molecular Evolution, Faculty of Mathematics and Natural Sciences, Heinrich Heine University Düsseldorf, 40225 Düsseldorf, Germany
Tel: +49 211 811 2343
E-mail: manon.schlikker@hhu.de

Manon L. Schlikker and Nadja K. Hoffmann contributed equally to this work.

(Received 14 January 2026, revised 23 June 2026, accepted 16 September 2026)

doi:10.1111/febs.70737

Phosphate is central to modern bioenergetics and to all theories for the origin of life. How phosphate entered metabolism is unknown, though microbial physiology and geochemical environments can provide important clues. Some bacteria obtain electrons and energy from phosphite (HPO_3^{2-}), a reduced form of phosphate (HPO_4^{2-}), that naturally occurs in serpentinizing (H_2-producing) hydrothermal systems. Here we show that the insoluble, solid-state catalyst native palladium, which is naturally deposited in serpentinizing hydrothermal systems, catalyzes the oxidation of phosphite to phosphate and H_2 in water at 25–100 °C in a highly exergonic reaction. Palladium awaruite (Pd_xNi_3Fe), a common form of Pd^0 in serpentinizing vents, also catalyzes phosphite-dependent phosphorylation. Phosphite oxidation over Pd^0 generates a reactive but so far unidentified chemical intermediate, possibly metaphosphate, $[PO_3]^-$, that readily phosphorylates hydroxyl moieties in glycerol, ribose, glucose, serine, and cytidine at 25–100 °C in 2–72 h. The same conditions also generate (i) phosphoanhydride bonds in pyrophosphate, polyphosphates, and ADP, (ii) the phosphoramidate bond in phosphocreatine, (iii) and the acyl phosphate bond in acetyl phosphate, which is obtained overnight at 25 °C with 8% yield. The reactions proceed without sulfur, excluding thioester or metal sulfide intermediates. Phosphite-dependent phosphorylations under serpentinizing hydrothermal vent conditions are facile. They identify a natural, geochemical source of prebiotic phosphorylation and a novel source of metabolic energy at origins. The central role of phosphate in bioenergetics, metabolism, and nucleic acids could reflect metal-catalyzed, redox chemistry of phosphorus in the environment where metabolism (and life) arose.

Introduction

Theories for the origin of life hinge upon mechanisms for the incorporation of phosphate into organic compounds [1–3]. In genetics first theories [4,5], phosphate is an essential structural component of nucleic acid synthesis and replication, as RNA is ~30% phosphate by weight. In metabolism first theories [6–9], phosphate is a transient carrier of metabolic energy. It serves as a universal energy currency of cells, reacting with organic or organophosphate substrates to form metastable bonds [1] that release free energy upon hydrolysis. Phosphorylation activates molecules for further synthesis and couples energy release to otherwise endergonic reactions, pushing chemical reactions in the life process forward [10,11].

Abbreviations
AdpA, AMP-dependent phosphite dehydrogenase; EDS, energy-dispersive spectroscopy; ESI–LC–MS, electrospray ionization liquid chromatography–mass spectrometry; FA, formic acid; fcc, face-centered cubic; NMR, nuclear magnetic resonance; Q-TOF, quadrupole-time-of-flight; SEM, Scanning Electron Microscopy (SEM images); SLP, substrate-level phosphorylation; XRD, X-ray diffraction.

© 2026 The Author(s). *The FEBS Journal* published by John Wiley & Sons Ltd on behalf of Federation of European Biochemical Societies.
This is an open access article under the terms of the Creative Commons Attribution License, which permits use, distribution and reproduction in any medium, provided the original work is properly cited.

Possible environmental sources and states of phosphorus at origins are still debated [12,13]. In the biosynthesis of amino acids, nucleotides, and cofactors of modern cells, phosphorus exists exclusively as phosphate [14,15]. Phosphonates, compounds with a C–P bond, are synthesized and utilized by microbes [16,17], but not for ATP or nucleic acid synthesis [16,18]; they are synthesized from phospho*enol*pyruvate (a phosphate ester) without redox reactions [19] and they release phosphate upon degradation [18]. The most common phosphorus mineral in nature, calcium phosphate (apatite), is poorly soluble [20,21]. Phosphate is not readily incorporated into organic compounds via prebiotic syntheses without enzymes, requiring the use of nonphysiological conditions including oven-heating to dryness in the presence of condensing agents such as ammonia and urea [22,23], incubation with phosphate in pure formamide [24], strong nonphysiological electrophiles such as cyanoacetylene, cyanogen, cyanate, cyanoformamide, cyanamide [25], or highly reactive forms of phosphorus [26] such as P_4O_{10} [13]. These chemical impasses to phosphate incorporation are also known as the 'phosphate problem' [2], which has a long history [27] and persists to the present, as Weller *et al.* [13] recently summarized: '*a fundamental, universally accepted mechanism how early Earth could have provided phosphate for prebiotic chemistry remains unknown*'. Yet phosphorus was absolutely essential for metabolism, information, heredity and energy at origins, indicating that facile routes of prebiotic phosphorylation must have existed on the early Earth. How to find them?

We reasoned that microbial physiology [28] and the chemically reactive environments of hydrothermal vents [29] in particular serpentinizing (alkaline, H_2 producing) hydrothermal vents [30] can point to possible natural sources of phosphorylation. Schink *et al.* isolated bacteria that can use phosphite as their sole phosphorus source, converting it to phosphate via enzymatic phosphite oxidation [31–33], prompting the suggestion by Wolfgang Buckel [34] that phosphite could have generated acyl phosphates via phosphite oxidation at a biochemical origin. Though phosphite is vastly more soluble than phosphate, reports for its occurrence in modern natural environments are rare [17,35]. Yet phosphite-oxidizing genes are extremely common among modern microbes, with up to 1.5% of sequenced prokaryotes being able to utilize phosphite [36]. Phosphite was furthermore present in Archaean oceans [37] and in Archaean rocks [35].

Microbial genomes obtained from serpentinizing hydrothermal vents have an increased frequency of phosphite-oxidizing genes [38–40]. Moreover, Pasek *et al.* [41] measured the frequency of different phosphorus species in rock samples from formations altered by serpentinization and found that between 20% and 50% of the total phosphorus in some samples was phosphite, the remainder being phosphate. Why does phosphite occur in serpentinized rocks? Serpentinization is a geochemical process [42–44] in which water circulating 1–5 km in the Earth's crust is reduced by reactions with Fe(II) minerals, generating very high H_2 concentrations (often >10 mM) and very alkaline (pH 9–12) effluent [39]. The result is that the fluids in serpentinizing systems generate potentials up to −900 mV [45], sufficient to reduce dissolved transition metals to the native (zero valent, metallic) state [46] and, by inference, reduce phosphate to phosphite [41], as the midpoint potential of the HPO_4^{2-} to HPO_3^{2-} redox couple is −690 mV [31]. While phosphite itself has not yet been reported in the effluent of hydrothermal vents, its presence in serpentinized rocks [41] and the frequency of phosphite-oxidizing genes in microbes of serpentinizing systems [38–40] prompted us to investigate its ability to phosphorylate organic compounds using conditions (aqueous, alkaline) and catalysts germane to serpentinizing vents.

As catalysts for phosphite activation, we focused on native transition metals, because (i) native metals are naturally deposited in serpentinizing hydrothermal systems [46] and because (ii) under aqueous conditions, native transition metals have been found to readily convert H_2 and CO_2 to organic acids [47–49], convert NH_3 and organic acids to amino acids [50,51], convert H_2 and CO_2 to long chain hydrocarbons [52], to functionally interact with NAD^+ [53,54], pyridoxal [51], and ferredoxin [55], and to reduce double bonds of biochemical compounds [56]. In an initial screen [15], we found that Pd^0, a metal that occurs in the native state in serpentinizing hydrothermal vents [57–59], was more effective than Fe^0, Co^0, Ni^0, or Ni_3Fe in the oxidation of HPO_3^{2-} to HPO_4^{2-}. Hence, we probed the ability of HPO_3^{2-} over Pd^0 in water to phosphorylate biochemicals under prebiotic conditions.

Results

Mao *et al.* [33] characterized the enzyme that the bacterium *Phosphitispora fastidiosa* uses to access electrons and generate ATP from phosphite: AMP-dependent phosphite dehydrogenase (AdpA). AdpA catalyzes the reaction $AMP + HPO_3^{2-} + NAD^+ \rightarrow ADP + NADH$, whereby ADP is subsequently converted to ATP via adenylate kinase: $2ADP \rightarrow ATP + AMP$. The enzyme does not harbor a metal cofactor. The oxidation of HPO_3^{2-} via the reaction HPO_3^{2-}

© 2026 The Author(s). *The FEBS Journal* published by John Wiley & Sons Ltd on behalf of Federation of European Biochemical Societies.

+ $H_2O \rightarrow HPO_4^{2-} + H_2$ is exergonic with $\Delta G_0' = -46.3$ kJ·mol^{-1} [60]. In water, Pd^0 oxidizes HPO_3^{2-} to HPO_4^{2-}, generating H_2 during the reaction. In the presence of AMP, the palladium-catalyzed reaction is AMP + $HPO_3^{2-} \rightarrow$ ADP + H_2, with 4.3% conversion after 2 h and 5.9% conversion after 18 h at 50 °C (Fig. 1A, Fig. S1A–J, Table S1). The ADP product was identified using ^{1}H NMR (black line, Fig. 1B) by comparison to the library standard (blue area, Fig. 1B) and using ^{31}P NMR, with specific peaks for adenosine 5′-diphosphate at −6 and −10.4 ppm (Fig. 1C). ADP yields decrease with temperature, with breakdown to AMP + P_i and adenosine (not shown). Though far less efficient than AdpA, Pd^0 (as Pd^0 on carbon, Pd/C) replaces the AdpA enzyme for phosphite to phosphate (in ADP) oxidation and uses H^+ instead of NAD^+ as the electron acceptor, generating H_2 instead of NADH.

In metabolism, the 5′-phosphate of nucleotides stems from 5-phosphoribosyl-1-pyrophosphate, while prebiotic-type nucleotide syntheses typically involve nucleoside phosphorylation. Phosphite over Pd^0 phosphorylates cytidine, in addition to other positions, at the 5′ position to cytidine 5′-monophosphate at 30 °C in 72 h, albeit at low yields of ca. 0.37% in ^{1}H NMR spectra (Fig. 1D, Fig. S2A–G, Table S2). Though our yields are an order of magnitude lower than those obtained using phosphate to phosphorylate uridine in the presence of molar concentrations of cyanogen, cyanoformamide, cyanate, cyanamide, thioformate, ethylisocyanide, and a carbodiimide [22,25], our reaction requires no organic additives, only phosphite and water, plus an effective solid state transition metal catalyst. Because readers unfamiliar with heterogeneous catalysis might be concerned about the concentration of Pd^0 in our reactions, we clarify that our Pd^0 catalyst is not dissolved; it is in the solid phase and has a concentration of zero, the same concentration as glass from the walls of vials in which our reactions are performed. AMP phosphorylation using 75 mM HPO_3^{2-} over Pd/C, instead of 200 mM, 50 °C, 72 h, generated a yield of 0.7% (Fig. S1).

Hydroxyl groups

In modern metabolism, sugar phosphates are essential for the biosynthesis of amino acids, nucleic acids, reserve polysaccharides, and cell wall components. In autotrophs that use the acetyl-CoA pathway, ribose 5-phosphate is generated through gluconeogenesis [61] and the oxidative pentose phosphate pathway [62]. Nonenzymatic phosphorylation of sugars can be attained through heating with phosphate and condensing agents such as cyanogen or cyanamide [25], but

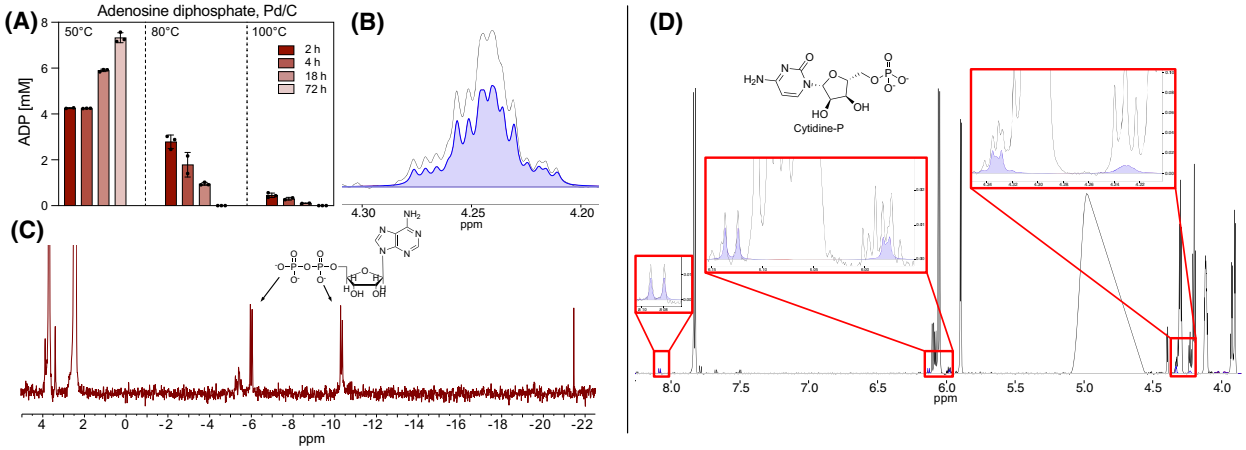

Fig. 1. Palladium-catalyzed phosphorylation of AMP and cytidine using phosphite. (A) Formation of adenosine diphosphate (ADP) from AMP (100 mM) and phosphite (200 mM) in the presence of Pd/C (1.5 mmol) under 5 bar Ar at pH 9, reaction volume 1.5 mL. Reaction temperatures were 50 °C, 80 °C, and 100 °C stopped after 2 h, 4 h, 18 h, and 72 h. ADP concentrations were estimated by ^{1}H NMR integration (Fig. S1, Table S1). Data are shown as mean ± SD of $n = 3$ independent experiments. (B) Representative ^{1}H NMR spectrum from one of $n = 3$ independent experiments (black) of the 50 °C, 72 h reaction, showing a diagnostic ADP signal at ~4.25 ppm; purple overlay represents the internal library reference. (C) Representative ^{31}P NMR spectrum from one of $n = 3$ independent experiments of the same sample, showing ADP peaks at −6 ppm and −10.4 ppm. (D) Representative ^{1}H NMR spectrum from one of $n = 2$ independent experiments of cytidine (100 mM) reacted with phosphite (200 mM) under identical conditions (Pd/C, 50 °C, 72 h, pH 9, 5 bar Ar), showing signals consistent with the formation of cytidine monophosphate (CMP; purple insets). That this product contains the cytidine 5-phosphate isomer was shown by electrospray ionization liquid chromatography–mass spectrometry analysis (Fig. S2, Table S2).

© 2026 The Author(s). *The FEBS Journal* published by John Wiley & Sons Ltd on behalf of Federation of European Biochemical Societies.

the existence of highly reactive nitrile-containing compounds such as cyanogen or cyanamide on the early Earth is uncertain at best [63] while the existence of serpentinizing systems on the early Earth is certain [64–66]. Pd/C catalyzes the phosphorylation of ribose to ribose 5-phosphate, in addition to other positions, at 0.6% yield (Fig. 2A, Fig. S3A–E, Table S2). The yield is comparable to that obtained through heating ribose and phosphate with cyanamide [25,67], a procedure that is also used to phosphorylate glucose [25,68]. Phosphite with Pd/C generates glucose phosphate (Fig. 2B, Fig. S4A–F, Table S1) at yields of 1.1% (at least 10-fold lower than the classical cyanogen method), but in pure water, without the requirement for addition of cyanogen gas or cyanamide [67,68], and at a concentration of 1.1 mM, slightly lower than the physiological concentration of glucose 6-phosphate in *E. coli* grown on glucose, 1.5 mM [69].

Although it is possible, if not probable, that the lipids of bacteria and archaea were synthesized by enzymatic processes in early evolution [9,70], glycerol phosphate was required for phospholipid synthesis. Glycerol phosphorylation has been reported using schreibersite, Fe_3P, a highly reactive phosphide that occurs in meteorites [71]. With HPO_3^{2-} and Pd/C in water, glycerol is readily phosphorylated with 0.8% yield after 4 h and 1.7% yield after 72 h at 50 °C, with slightly lower yields at higher temperatures (Fig. 3A–C, Fig. S5A–H, Table S1). The hydroxyl group of serine is very efficiently phosphorylated over Pd/C with ca. 49.5% yield after 18 h and 50 °C (Fig. 3D,F,G, Fig. S6A–H, Table S1), and lower yields at higher temperatures. Using Pd^0 nanoparticles, without carbon support, serine phosphorylation yield is generally lower, but increases with time and temperature (Fig. 3E, Fig. S7A–F, Table S1).

High-energy bonds

A key to phosphate in energy metabolism is its ability to form generally long, readily attacked (and hydrolyzed) metastable bonds with various moieties [72]. Hydrolysis of such bonds releases free energy that can be harnessed for phosphorylation of other compounds or enzymatically coupled to endergonic reactions, rendering the coupled reaction exergonic [11]. The free energy of hydrolysis for some bioenergetically relevant reactions under standard physiological conditions (25 °C, pH 7) is given in Table 1. In cells, high-energy phosphate bonds are synthesized as ATP through the stoichiometric coupling of enzymatic reactions to ATP synthesis via substrate-level phosphorylation (SLP) [10,76] or from chemiosmotic coupling through the harnessing of ion gradients via rotor-stator ATPases [76,77].

Before enzymes, SLP and chemiosmotic harnessing via ATP synthases did not exist. Metabolic reactions are continuous in nature. What was the continuous

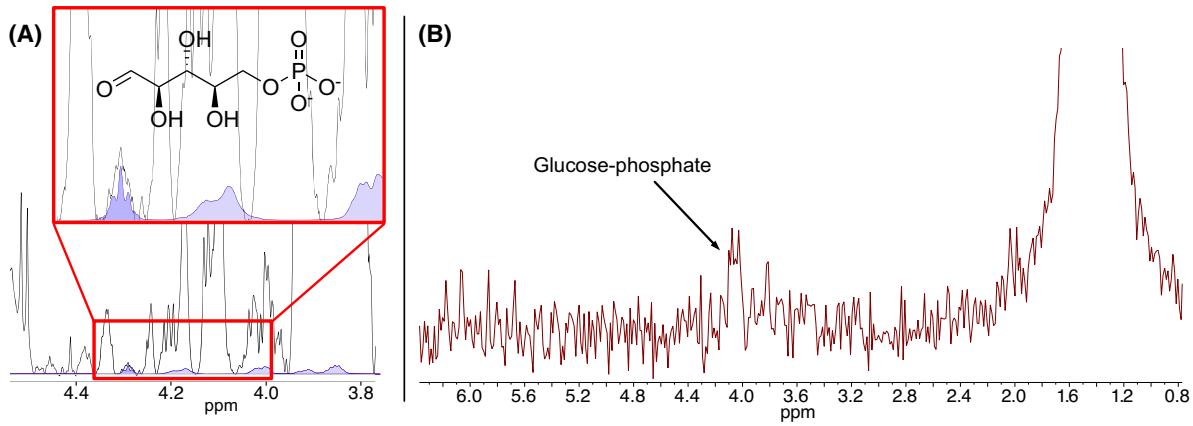

Fig. 2. Pd/C-catalyzed phosphorylation of ribose and glucose using phosphite as phosphate donor. (A) Representative ^{1}H NMR spectrum from one of $n = 2$ independent experiments of the 50 °C, 72 h ribose (100 mM) and phosphite (200 mM) reaction in the presence of Pd/C (1.5 mmol) under 5 bar Ar at pH 9 in a total reaction volume = 1.5 mL. Ribose phosphate was detected by ^{31}P NMR at 50 °C after 18 h and 72 h, showing a characteristic ribose phosphate signal at ~4.28 ppm. That this product contains the ribose 5-phosphate isomer was shown by electrospray ionization liquid chromatography–mass spectrometry analysis (Fig. S3, Table S2). (B) Representative ^{31}P NMR spectrum from one of $n = 2$ independent experiments of the glucose phosphorylation reaction (100 mM glucose, 200 mM phosphite, 1.5 mmol Pd/C, 40 °C, 18 h) under Ar at pH 9, with a phosphate resonance consistent with glucose phosphate at ~3.9 ppm (Fig. S4), without specifying the isomer.

© 2026 The Author(s). *The FEBS Journal* published by John Wiley & Sons Ltd on behalf of Federation of European Biochemical Societies.

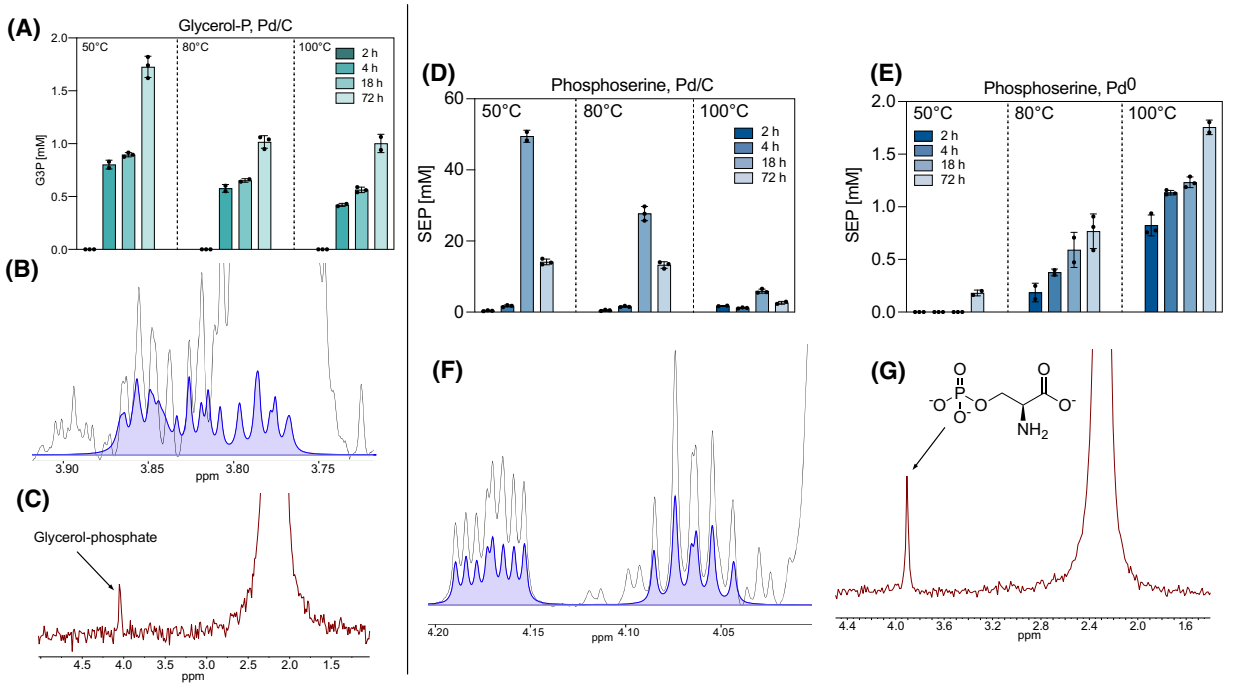

Fig. 3. Phosphorylation of glycerol and serine by phosphite in water. (A–C) Glycerol phosphate formation from 100 mM glycerol and 200 mM phosphite over 1.5 mmol Pd/C in water under Ar at pH 9, reaction volume 1.5 mL. (A) Glycerol phosphate yield at 50 °C, 80 °C, and 100 °C after 18 h and 72 h (Fig. S5, Table S1). Data are shown as mean ± SD of $n = 3$ independent experiments. (B) Representative ^{1}H NMR spectrum from one of $n = 3$ independent experiments of the 50 °C, 72 h reaction (black), overlaid with internal library standard (purple). (C) Representative ^{31}P NMR spectrum from one of $n = 3$ independent experiments of the same sample shows a characteristic peak for glycerol phosphate. (D–G) Phosphorylation of 100 mM serine under identical conditions. (D) Serine phosphorylation yield using Pd/C (Fig. S6, Table S1). Data are shown as mean ± SD of $n = 3$ independent experiments. (E) Yield with native Pd^{0} nanoparticles (Fig. S7, Table S1). Data are shown as mean ± SD of $n = 3$ independent experiments. (F) Representative ^{1}H NMR spectrum from one of $n = 3$ independent experiments of the Pd/C reaction after 18 h at 50 °C (black) and internal standard (purple). (G) Representative ^{31}P NMR spectrum from one of $n = 3$ independent experiments of the same sample confirms the presence of phosphoserine.

Table 1. Free energy of hydrolysis for selected reactions.

Hydrolysis reaction	$\Delta G_0'$	Ref.
PEP + H_2O → HPO_4^{2-} + pyruvate	−62	73
1,3-BPGA + H_2O → HPO_4^{2-} + 3PGA	−52	73
HPO_3^{2-} + H_2O → HPO_4^{2-} + H_2	−46	60
ATP + H_2O → AMP + pyrophosphate	−46	73
Creatine-P + H_2O → HPO_4^{2-} + creatine	−43	73
Acetyl-P + H_2O → HPO_4^{2-} + acetate	−43	73
Carbamoyl-P + H_2O → HPO_4^{2-} + carbamate	−39	73
Acetyl-CoA + H_2O → CoASH + acetate	−32	74
ATP + H_2O → HPO_4^{2-} + ADP	−31	11
Glucose 1-P + H_2O → HPO_4^{2-} + glucose	−21	73
Pyrophosphate + H_2O → 2 HPO_4^{2-}	−20	73
Glucose 6-P + H_2O → HPO_4^{2-} + glucose	−14	73
Glycerol 2-P + H_2O → HPO_4^{2-} + glycerol	−9	73

The value of $\Delta G_0'$ for the phosphite-oxidizing reaction shown has also been reported as ca. –55 kJ·mol^{-1} [75].

source of high-energy bonds at metabolic origin? In water, HPO_3^{2-} over Pd/C phosphorylates acetate, generating acetyl phosphate (Fig. 4A,B, Fig. S8A–D) with a yield of 8%. The acyl phosphate bond in acetyl phosphate has a free energy of hydrolysis $\Delta G_0' = -43$ kJ·mol^{-1} (Table 1), sufficient to phosphorylate a variety of substrates including ADP to ATP via SLP [11]. In water, HPO_3^{2-} over Pd/C also phosphorylates creatine, generating the phosphoamidate bond in phosphocreatine (Fig. 4C, Fig. S9A–E, Table S2) which also has a free energy of hydrolysis $\Delta G_0' = -43$ kJ·mol^{-1} (Table 1). Phosphocreatine is a phosphagen that is used as a reservoir of high-energy bonds to rapidly synthesize ATP in muscle via the enzyme creatine kinase. A role for creatine and other phosphagens in prebiotic chemical evolution now appears possible. In water, HPO_3^{2-} over Pd/C also phosphorylates phosphate to form pyrophosphate (Fig. 4D). Pyrophosphate is traditionally considered as a primordial energy currency [10], but it has a lower free energy of hydrolysis than glucose 1-phosphate (Table 1) and is more likely a currency of irreversibility [79,80] than energy.

© 2026 The Author(s). *The FEBS Journal* published by John Wiley & Sons Ltd on behalf of Federation of European Biochemical Societies.

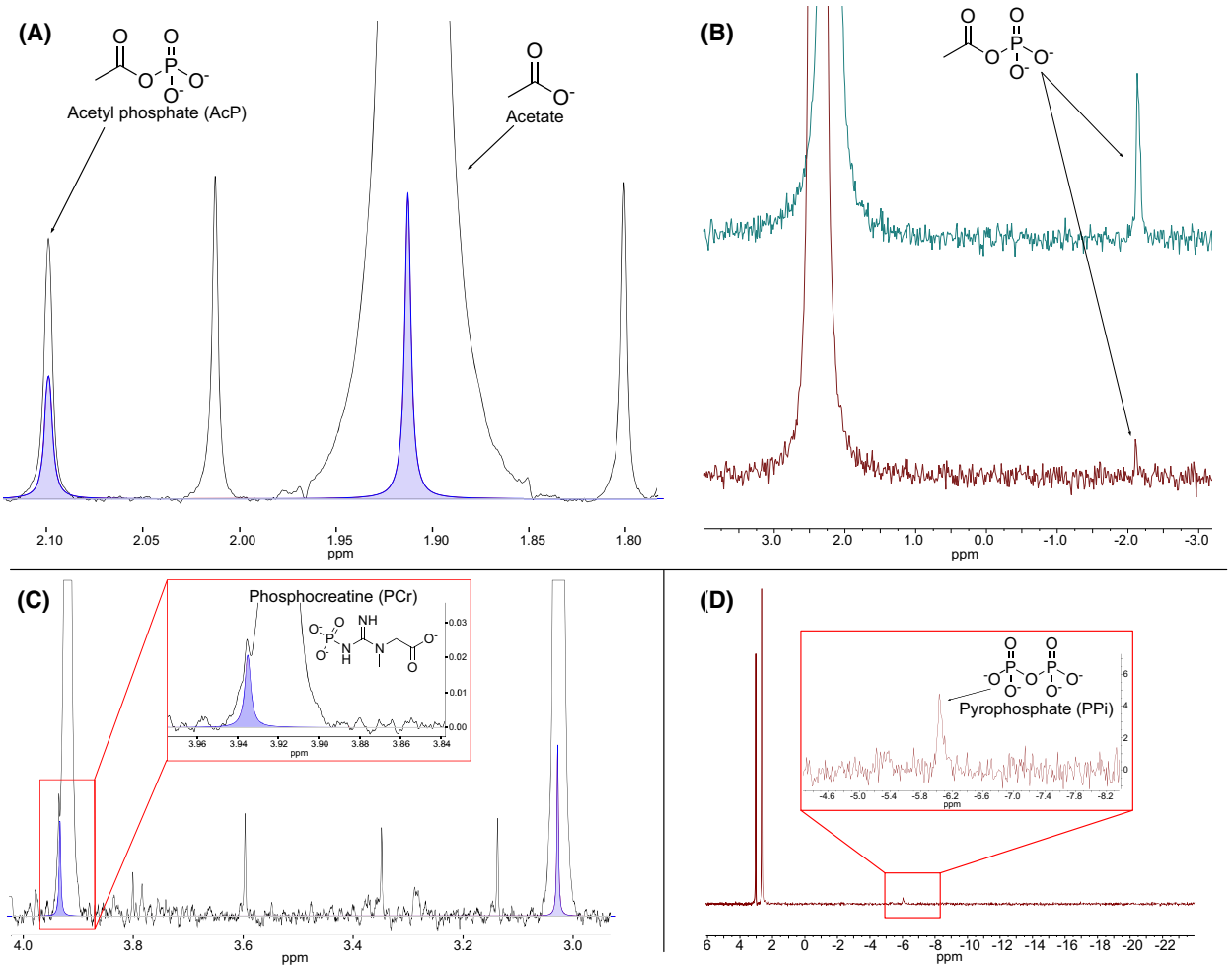

Fig. 4. Formation of energy-rich phosphoanhydrides via Pd/C-catalyzed phosphite oxidation. (A) Representative ^{1}H NMR spectrum from one of $n = 3$ independent experiments of a reaction containing acetate (100 mM) and phosphite (200 mM) with Pd/C (1.5 mmol) in 1.5 mL water under 5 bar Ar at pH 9 after 18 h at 25 °C. Two natural abundance ^{13}C acetate satellite peaks appear at 2.02 and 1.8 ppm [78]. (B) Representative ^{31}P NMR spectra from one of $n = 3$ independent experiments showing acetyl phosphate (AcP) identification via co-injection. Top: reaction sample spiked with AcP (cyan); bottom: unspiked reaction mixture (red), confirming identity (Fig. S8). (C) Representative ^{1}H NMR spectrum from showing formation of phosphocreatine (PCr) from creatine (100 mM) and phosphite (200 mM) under identical conditions with Pd/C (1.5 mmol) at 60 °C for 18 h (black trace), confirmed by overlay with the Chenomx library reference (purple) (Fig. S9, Table S2). (D) Representative ^{31}P NMR spectrum from of a reaction (200 mM phosphite) at 80 °C after 18 h, showing pyrophosphate (PPi) formation. Signals for residual phosphate (Pi) and unreacted phosphite (Pt) are also visible.

The synthesis of pyrophosphate (Fig. 4D) suggests that further phosphate phosphorylations are possible with HPO_3^{2-} over Pd/C. We observe the synthesis of polyphosphate (Fig. 5A) and, surprisingly in our view, trimetaphosphate (Fig. 5B). Polyphosphates are very common among bacteria and archaea and are commonly viewed as a potential energy reserves and phosphate storage compounds [81,82]. That HPO_3^{2-} can generate polyphosphates over Pd in water suggests that these have been in existence since phosphate was first used as an energy currency. More surprising was the detection of trimetaphosphate, yet the ^{31}P NMR signal observed in Fig. 5B is identical to that reported by Gull *et al.* [83]. Trimetaphosphate ($P_3O_9^{3-}$) is not known from cells but is widely used as a phosphorylating agent in prebiotic chemistry [84]. That trimetaphosphate is formed in addition to a broad range of physiological phosphorylated products suggests that it could have served as a phosphorylating agent in early biochemistry. We cannot presently exclude the

© 2026 The Author(s). *The FEBS Journal* published by John Wiley & Sons Ltd on behalf of Federation of European Biochemical Societies.

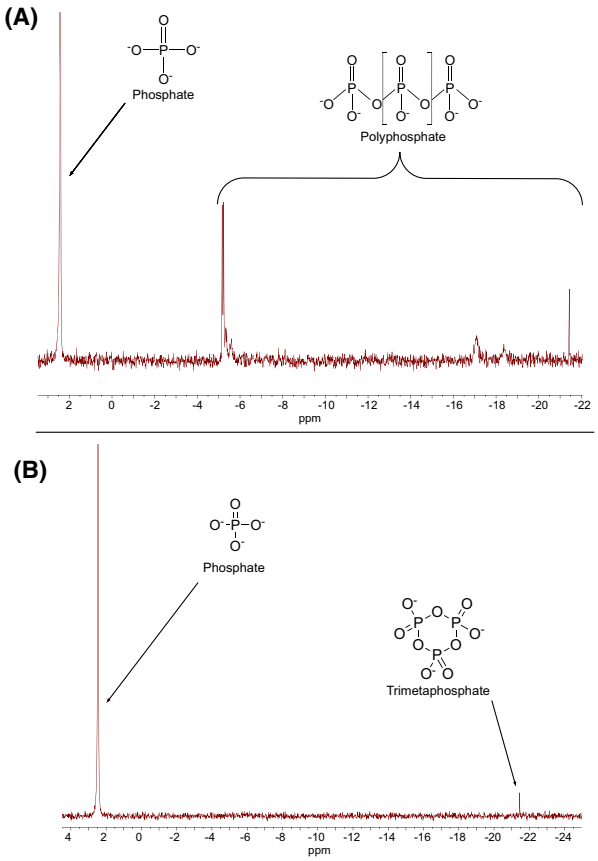

Fig. 5. Formation of linear and cyclic condensed phosphates by phosphite oxidation over Pd/C. (A) Representative ^{31}P NMR spectrum from of a reaction containing 200 mM phosphite and 1.5 mmol Pd/C at 80 °C for 18 h under 5 bar Ar at pH 9, reaction volume = 1.5 mL, showing the formation of linear polyphosphates in addition to phosphate. (B) ^{31}P NMR spectrum of a parallel reaction performed under 50 °C at 18 h reveals the formation of trimetaphosphate, a cyclic triphosphate species, alongside residual phosphate.

possibility that trimetaphosphate might be involved as a transient, undetected intermediate in some of the phosphorylation reactions we report here.

Phosphite-dependent phosphorylations over Pd generate H_2. Does H_2 inhibit the phosphite oxidation reaction? We performed the oxidation reaction in the presence of 10 bar H_2 instead of 5 bar Ar (Fig. S10A,B). The result shows that the reaction still proceeds, but with 62% lower yield (38% instead of 100% conversion). High partial pressure of H_2 thus slows the phosphite oxidation reaction but does not inhibit it completely. During the present work, we observed that reactor headspace pressure increased by amounts corresponding to stoichiometric H_2 formation during phosphate formation according to $H_2O + HPO_3^{2-} \rightarrow HPO_4^{2-} + H_2$ with $\Delta G_0' = -46$ kJ·mol^{-1} [60].

In modern serpentinizing hydrothermal systems, Pd^0 typically occurs as Pd-awaruite [57–59], while our present reactions are catalyzed by Pd^0 supported on carbon. Therefore, we synthesized Pd-awaruite as 5% by weight Pd in Ni_3Fe and tested its ability to phosphorylate AMP. This Pd-awaruite catalyst was obtained through the one-step calcination/reduction of nickel, iron, and palladium nitrate precursors under H_2/Ar, ensuring the formation of the target alloy phase. The X-ray diffraction (Fig. S11A, Table S3) confirmed formation of a highly crystalline alloy phase with face-centered cubic (fcc) structure, similar to Ni_3Fe phase (JCPDS no. 88–1715). Sharp reflections indicate the formation of larger crystallite sizes, while no additional PdO-related phases or other phase impurities were detected. Further, scanning electron microscopy coupled with energy-dispersive spectroscopy (SEM-EDS) revealed a homogeneous distribution of Ni, Fe, and Pd, with a composition close to the intended formulation (wt%: Ni = 66%, Fe = 29%, Pd = 5%) (Fig. S11B, Table S3). SEM imaging also confirms the presence of large sintered particles with intraparticle porosity.

© 2026 The Author(s). *The FEBS Journal* published by John Wiley & Sons Ltd on behalf of Federation of European Biochemical Societies.

The catalytic results are shown in Fig. 6A,B (Fig. S12A,B). 5% Pd-Ni_3Fe is effective as solid-state catalyst, indicating that the most common form of Pd identified so far in serpentinizing systems, Pd-awaruite, also catalyzes phosphorylation reactions via HPO_3^{2-} oxidation.

Possible mechanism

What is the phosphorylating agent? We have no direct evidence for the nature of reaction intermediates in these phosphorylations, but the products we observe are consistent with a proposal for the course of phosphite-dependent phosphorylation over Pd as outlined in Fig. 7. The proposal involves solid-state transition metal (native palladium) catalysis as the phosphite-activating step and thus differs from the acyl phosphite-dependent mechanism proposed by Buckel [34].

The proposed mechanism is based in part on the proposed mechanism for *Phosphitispora fastidiosa* AdpA [33] (hydride removal) and the dissociative mechanism proposed for *Bacillus* sp. phosphite oxidase [85], but also in part on the observations (1) that implicate metaphosphate in acyl phosphate [86] and enzymatic phosphoester hydrolysis [87], (2) that some phosphorylating and dephosphorylating enzymes have been shown to generate a planar metaphosphate intermediate, identifiable in crystal structures of fructose-1,6-bisphosphatase [88], in quantum mechanical studies of phosphoserine phosphatase [89] and in mechanistic studies of phosphoglucomutase [90]. The accumulation of trimetaphosphate and polyphosphates in our experiments (Fig. 5) would be compatible with a highly reactive [91] metaphosphate intermediate. The scheme proposed in Fig. 7 should, in principle, be reversible, but the equilibrium lies on the side of phosphate in the presence of water (R = H), with low concentrations of phosphorylated compounds (R = alkyl, phosphoryl, acyl).

Discussion

One general solution to the 'phosphate problem' is the suggestion from origins research [92], microbial physiology [31,34,39], geochemistry [3,35,37,41], environmental genomics [38,40], and planetary science [41] that reduced forms of phosphorus were the source of phosphorylation at origins. Yet biochemically meaningful, physiologically compatible, and geochemically realistic phosphorylation reactions using phosphite or other reduced phosphorus compounds have been lacking. We report such reactions, though we are not the first to describe nonenzymatic phosphorylation with phosphite.

Gull *et al.* [93] showed that diphosphite reacts with NH_3 to generate amidophosphite, which can be oxidized with strong oxidants (O_2, H_2O_2, or ClO^-) to phosphorylate organic compounds in the presence of urea, though these strong oxidants were, in standard accounts, not present on the early Earth. Using phosphite under wet-dry cycles in the presence of air (21%

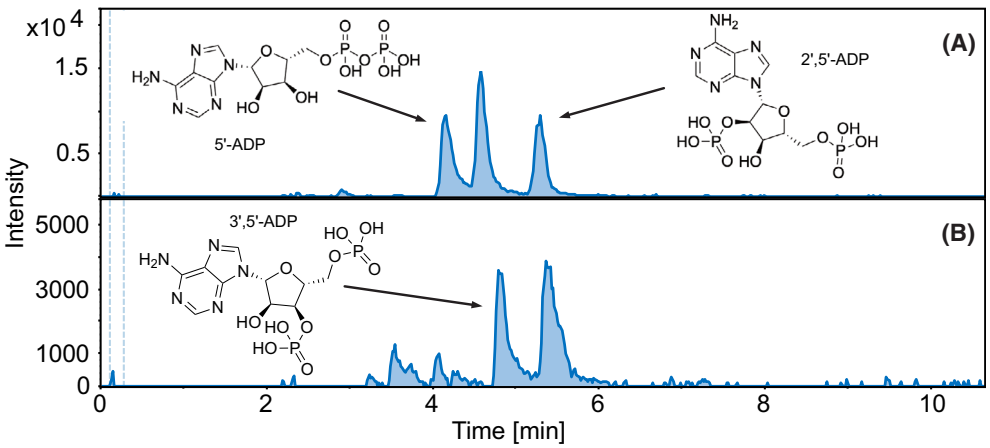

Fig. 6. Formation of ADP via phosphite-dependent phosphorylation over Pd–Ni_3Fe catalysts under varying conditions. (A, B) All experiments were performed with 100 mM AMP, 200 mM phosphite, a reaction time of 96 h, and 1.5 mmol catalyst (Fig. S12). The spectra shown are from single experiments ($n = 1$). (A) Reaction with 5% Pd–19% Ni_3Fe at 50 °C, showing the formation of ADP from AMP with multiple peaks corresponding to different phosphorylation sites. (B) Reaction performed at 100 °C with 5% Pd–19% Ni_3Fe. The different ADP isomers are depicted in their protonated forms. The yield of ADP (μM) for all three isomers combined is A: 13.7 and B: 3.8, with relative proportions of each isomer given in Table S3.

© 2026 The Author(s). *The FEBS Journal* published by John Wiley & Sons Ltd on behalf of Federation of European Biochemical Societies.

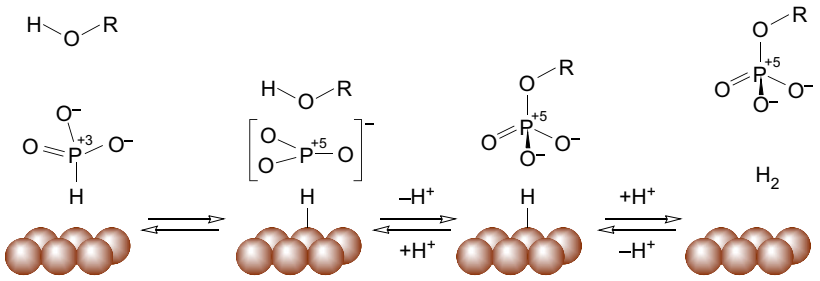

Fig. 7. Proposed mechanism for phosphite-dependent phosphorylation on metal surfaces. A schematic proposal for the course of phosphite-dependent phosphorylation: oxidative hydride removal, intermediate formation (metaphosphate shown as a possibility), P–O bond formation (P–N bond formation in the case of phosphocreatine), H_2 formation.

O_2) and with the addition of urea, Gull *et al.* [94] reported phosphorylation and phosphonylation of hydroxyl groups on organic compounds. Among their products they reported glycerol 1-phosphate, glycerol 2-phosphate, glycerol 1-phosphite, glycerol 2-phosphite, 5′-adenosine phosphite, 5'-AMP, 2′ and 3′-adenosine phosphites, as well as 2′- and 3'-AMP in addition to 2′-, 3′- and 5′- uridine phosphites. Among their inorganic reaction products, they observed phosphate, pyrophosphate, pyrophosphite, and isohypophosphate. The drying method for phosphite with urea as a condensing agent, as is traditionally used for phosphate activation [25], yields mainly organic phosphites [94]. Instead of condensing agents, we used a transition metal catalyst, one that naturally exists at serpentinizing hydrothermal vents where phosphite is formed, and water as the oxidant. We observed phosphorylated organic products and phosphorylated inorganic products, indicating that phosphite is oxidized on the catalyst surface prior to reaction with phosphorylation substrates (or water), in line with our proposal for transient metaphosphate formation during the reaction as in Fig. 7.

Our report is also not the first to demonstrate acetyl phosphate formation in a prebiotic context. Lohrmann and Orgel [22] obtained acetyl phosphate from reactions of phosphate with ketenes, highly reactive compounds with the general structure $R_2C{=}C{=}O$, under nonphysiological conditions that, like ketenes themselves, are unlikely to have existed in life-giving quantities on an early Earth covered with rocks and water [65]. Whicher *et al.* [95] also obtained acetyl phosphate, but from reactions of thioacetate with phosphate, whereby (i) thioacetate itself is typically synthesized from the reaction of H_2S with organic anhydrides [96] and (ii) a convincing prebiotic synthesis of thioacetate is yet to be reported. More recently, Chen *et al.* [97] reported aqueous phosphorylation of acetate using diamidophosphate with sodium nitrite in a reaction driven by N_2 release, whereby diamidophosphate is a strong, but nonphysiological phosphorylating agent [98]. Pasek *et al.* [71] reported the phosphorylation of acetate using schreibersite, $(Fe, Ni)_3P$, a reactive and corrosive phosphorous species that occurs in meteorites but that is not known in terrestrial chemistry. Schreibersite generates radicals and the reaction products reported [71] included nonphysiological compounds resulting from a radical based (one-electron) mechanism that attacked the methyl group of acetate, rather than the carboxyl. In microbes, phosphite oxidation is NAD^+-dependent [33], hence a two-electron, hydride transfer reaction. Our reaction products (Figs 1–6) are well-known phosphorylated compounds from metabolism; our proposed reaction scheme (Fig. 7) involves hydride transfer.

A summary of our present findings (Table 2) reveals that a single phosphorylation system in water, Pd^0/HPO_3^{2-}, can phosphorylate a broad spectrum of biologically relevant substrates at their physiological positions. Notably, these reactions *conserve a portion of the energy* in the phosphite oxidation reaction ($\Delta G_0' = -46$ kJ·mol^{-1}), either as bonds with sufficient group transfer potential to phosphorylate ADP (e.g., acetyl phosphate or phosphocreatine), or as bonds with sufficient free energy of hydrolysis to promote further reaction. One might interpret Table 2 as evidence that Pd/HPO_3^{2-} generates excellent phosphorylating agents, such as ADP, phosphocreatine, or acetyl phosphate, but our interpretation is more direct: Pd/HPO_3^{2-} *is* the phosphorylating agent. In the most direct interpretation, Pd/HPO_3^{2-} represents the primordial source of phosphorylation and phosphate as the energy currency of life [1], present from the very beginning of prebiotic chemistry, long before the origin of enzymes, substrate level phosphorylation (SLP),

© 2026 The Author(s). *The FEBS Journal* published by John Wiley & Sons Ltd on behalf of Federation of European Biochemical Societies.

Table 2. Phosphite-dependent phosphorylations using Pd/HPO_3^{2-} in water.

Reactant	Product	Time [h]	Temp [°C]	Yield [%]	$\Delta G_0'$ hydr. [kJ·mol^{-1}][a]
Acetate	Acetyl-P	18	25	8	−43
Creatine	Phosphocreatine	18	60	0.002	−43
AMP	ADP	72	50	7.3	−31
AMP[c]	ADP	72	50	0.013	−31
Phosphite	Trimetaphosphate	18	80	~1[d]	−29[b]
Ribose	Ribose-P	72	30	0.6	−23
Glucose	Glucose-P	18	40	1.1	−21
Phosphite	Pyrophosphate	18	80	~1[d]	−21
Cytidine	Cytidine monophosphate	72	30	0.37	−14
Serine	Phosphoserine	18	50	49.5	−12
Glycerol	Glycerol-P	72	50	1.7	−9

[a]Free energy of hydrolysis of the respective organophosphate bond in the reaction product, values from this work and the literature. For $HPO_3^{2-} + H_2O \rightarrow HPO_4^{2-} + H_2$, $\Delta G_0' = -46.3$ kJ·mol^{-1} [60]; [b]Meyerhoff *et al.* [99] reported the free energy of hydrolysis of trimetaphosphate to three orthophosphate molecules as −88 kJ·mol^{-1} or −29.3 kJ·mol^{-1} per metaphosphate bond. If several reactions for the same substrate were performed, the conditions with the highest yield are given; [c]This reaction was performed using 5%Pd in Ni_3Fe (Fig. 6), all other reactions in the table refer to Pd/C catalyst; [d]Small specific peak in ^{31}P NMR, detection limit ca. 1% conversion.

ATP, or gradient harnessing ATP synthases [9]. Once early evolving chemical systems and LUCA [15,100] had invented the basic enzymatic machinery of bioenergetics, phosphorylation via HPO_3^{2-} and solid-state metals was replaced by energy metabolism in its modern state: ion pumping via redox reactions coupled to the plasma membrane with ATP synthesis via rotor stator ATP synthases and enzymatic SLP.

Though our yields are typically in the low % range, the concentrations of organophosphates obtained are similar to those observed in the cytosol of growing *E. coli* cells and the process we are modeling here is a serpentinizing hydrothermal vent, a (natural) continuous flow reactor system, in which organics are continuously synthesized from H_2, CO_2, and NH_3 (for a recent overview, see [56]). In the hydrothermal vent model, environmental phosphite is continuously supplied at steady state concentrations and is activated (oxidized) for phosphorylation reactions catalyzed by immobile solid--state catalysts, continuous supply over time counterbalancing modest batch yields in an origin context.

Without activation, phosphite is generally inert despite a large free energy of hydrolysis (Table 1) and a very negative midpoint potential (−690 mV [31]) and $\Delta G_0'$ (−46.3 kJ·mol^{-1} [60]) in the phosphite to phosphate conversion. Herschy *et al.* [35] estimated that phosphite, once formed, can resist environmental oxidation for thousands to millions of years, underscoring the need for catalysts to accelerate phosphite activation. The catalyst used here, native palladium, oxidizes phosphite to phosphate in water in hours (Figs 1–6) as opposed to millennia [35] or seconds for the NADH-forming enzymatic reaction catalyzed by AdpA [33]. Notably, Yang and Metcalf [60] reported that alkaline phosphatase from *Escherichia coli* rapidly oxidizes phosphite to phosphate in a H_2-producing reaction. An intermediate in the Pd-catalyzed reaction reported here forms phosphate bonds with oxygen and nitrogen atoms (Fig. 7); it is not known whether alkaline phosphatase [60] will phosphorylate organic substrates with phosphite. Nagaosa and Aoyama [101] reported the oxidation of phosphite to phosphate in aqueous solutions using Pd^0 and Pd/C in the presence of air (21% O_2). In our reactions without organics, the only available electron acceptors are protons in water, which form H_2. In the presence of organics, many residues other than H^+ could have become reduced during the reaction, because the midpoint potential of the phosphite to phosphate reaction is more negative than even the strongest reductants ($E_0 = -622$ mV) produced by nonphotosynthetic organisms [102]. However, we did not observe the reduction of organics, suggesting that the anaerobic oxidation reaction specifically generates metal-bound hydride and then H_2, rather than other reduction products, suggesting in turn that an oxidized intermediate is first generated during the phosphite oxidation reaction that subsequently phosphorylates available substrates (Fig. 7), rather than phosphite reducing them.

Several theories about biochemical evolution posit a central role for sulfur in primordial bioenergetics: The thioester world [103] and the iron–sulfur world [8]. In de Duve's theory [103], thioesters preceded phosphorylated compounds as the universal energy currency. In Wächtershäuser's theory, pyrite (FeS_2) formation preceded phosphate as the primordial energy currency [8]. Other theories posit primordial energetics provided by

© 2026 The Author(s). *The FEBS Journal* published by John Wiley & Sons Ltd on behalf of Federation of European Biochemical Societies.

reactions of diverse organosulfur compounds [104,105], in some formulations with no role at all for phosphate at the origin of metabolism [106]. A chemical theory posits cyanide, H_2S and energy from UV light at the origin of metabolism [107]. Contrary to sulfur-based theories for energy at origins, the reactions reported here generate the main carriers of biochemical energy in microbial metabolism—phosphoanhydrides and acyl phosphates—overnight in water in the complete absence of sulfur. Thus, neither thioesters, organosulfides, metal sulfides, nor H_2S are required for energy harnessing via phosphorylation in our experiments and by inference at metabolic origin. Furthermore, it now seems possible, if not likely and contrary to earlier proposals by one of us [9], that thioesters ($\Delta G_0' = -32$ kJ·mol^{-1}) were generated from acyl phosphates ($\Delta G_0' = -43$ kJ·mol^{-1}) in a prebiotic context, which would be more in line with their relative ranks among high-energy bonds (Table 1).

Theories that address the origin of phosphate-based energetics posit that substrate-level phosphorylation preceded chemiosmotic energy harnessing [9–11]. Our findings agree with that view. Moreover, serpentinizing hydrothermal vents are now known to generate the geochemical energy underlying both sources of high-energy phosphate bonds. It is known that serpentinization generates proton gradients of sufficient strength (1–3 pH units) and the right polarity (alkaline inside) to drive chemiosmotic ATP synthesis [9,108,109]. Consistent with that view, ATP synthase reconstituted into primordial-type vesicles consisting of primordial fatty acids alone can maintain a pH gradient of ~1 pH unit and drive ATP synthesis [110]. Phosphite-dependent phosphorylations are also a source of continuous and *geochemically supplied* chemical energy (Table 2), provided *for free* in the currency of metabolism—phosphorylation—by the environment of serpentinization and stemming from the highly exergonic nature of the phosphite oxidation reaction (Table 1). The environment needs to provide only water, Pd^0, phosphite, and substrates, without the need for condensing agents, diamidophosphates, phosphides, recurrent drying, UV light, or sulfur. The involvement of a metaphosphate intermediate in the reaction mechanism (Fig. 7) would be very much in line with Westheimer's arguments [1] in favor of a role for metaphosphate in biochemical phosphorylation reactions.

Spontaneous geochemical reactions under the aqueous conditions of serpentinizing hydrothermal vents now provide all three chemical energy currencies used in the metabolism of modern cells, continuously, and for free: (i) H_2 as a diffusible reductant for the generation of reduced ferredoxin [55], a key energy currency in anaerobes [76,111], (ii) harnessable chemiosmotic gradients [77] generated by the alkalinity of serpentinization effluent [9,110], and now (iii) substrate-level phosphorylation provided by phosphite and native metals naturally deposited in serpentinizing systems [46,57,58]. From the standpoint of phosphorylation and metabolic energy, this sets serpentinizing systems distinctly apart from all other chemical environments so far proposed as the site of life's origin. Our findings place Westheimer's question 'Why nature chose phosphates' [1] in new light: It now seems possible that phosphates were not *selected*; they were *accepted* as the main aqueous energy currency that the environment had in continuous supply, primordial energy metabolism being the outcome.

Methods

Reactions contained 100 mM of each organic substrate and 200 mM sodium phosphite (NaH_2PO_3; Merck, Sigma-Aldrich, St. Louis, USA) dissolved in distilled water and adjusted to a final volume of 1.5 mL. All organic substrates, product standards, and inorganic reagents were purchased from Merck, Sigma-Aldrich, unless stated otherwise. The pH was adjusted to 9.0. Palladium catalysts (Merck, Sigma-Aldrich) were weighed out outside a glovebox. Supported Pd/C (10 wt% Pd on activated carbon) was added at 159 mg per reaction, corresponding to approximately 0.15 mmol of elemental palladium. For comparison experiments, elemental palladium (Pd^0) was added at the same molar loading (0.15 mmol Pd). Catalyst loadings are reported as mmol of elemental Pd. Reaction mixtures were transferred into 3 mL glass vials, sealed with screw caps, and punctured with a sterile needle to allow pressure equilibration while maintaining a closed reaction environment. The vials were placed in a stainless-steel pressure reactor equipped with a temperature controller (Berghof BR-300 with BTC-3000). The reactor was purged three times with argon and subsequently pressurized to 5 bar Ar (99.999%). Reactions were conducted at 25, 30, 50, 80, or 100 °C for incubation times of 2, 4, 18, or 72 h, as specified for each experiment. After completion, the reactor was depressurized, and the vials were immediately transferred to 2 mL microcentrifuge tubes. Samples were centrifuged for 20 min at 16 060 ***g*** to separate the catalyst from the supernatant. The supernatants were collected for NMR analysis.

Synthesis and physicochemical characterization of the Pd-awaruite catalyst

Regarding the Pd-awaruite catalyst (5% Pd-Ni_3Fe), nickel, iron, and palladium nitrate precursors (Merck, Sigma-Aldrich) were mechanically ground and mixed before calcining/reducing them in a single step (20% H_2/Ar, 100 mL·min^{-1}, 1°C·min^{-1}, 550 °C, 8 h). After that, the catalyst was passivated by using 10% air/Ar mixture for 25 min. X-ray diffraction (XRD) pattern was recorded

© 2026 The Author(s). *The FEBS Journal* published by John Wiley & Sons Ltd on behalf of Federation of European Biochemical Societies.

using a PANalytical Empyrean X-ray diffractometer with a Bragg–Brentano configuration, and Cu Kα radiation as the X-ray source (λ = 0.1544 nm). The instrument was operated with a voltage of 45 kV and a current of 40 mA. The diffractogram was collected in the 2θ region defined between 20° and 80°. After acquisition, X'Pert HighScore Plus software was employed for the analysis and background subtraction. In order to identify the crystalline phases, JPCDS database patterns were used. Scanning Electron Microscopy (SEM images) were obtained with a field-emission Apreo 2 Scanning Electron Microscope from Thermo Fisher Scientific, Waltham, MA, USA. The working distance was maintained at approximately 5–10 mm, and the equipment was operated under high-vacuum conditions to achieve high-resolution imaging. Elemental analysis and mappings were obtained using Energy-Dispersive Spectroscopy (EDS) and Aztec Software.

NMR analysis of phosphorylation products

Both ^{31}P and ^{1}H NMR spectra were acquired at the Center for Molecular and Structural Analytics (CeMSA@HHU, Heinrich Heine University Düsseldorf). Organic phosphorylation products, glucose-P, glycerol-P, phosphoserine, and acetyl phosphate, were identified and quantified by ^{1}H NMR using the internal compound library of Chenomx NMR Suite. ^{31}P NMR spectroscopy was used to quantify phosphate formation and ADP production, and to monitor the formation of phosphorylated organic species. Quantification of phosphate and ADP was performed using calibration curves following the procedure described in Ref. [15]. For this purpose, concentration series of authentic standards were prepared in H_2O and mixed with DSS in D_2O prior to measurement under identical conditions as the experimental samples. Linear regression analysis yielded the calibration equations $y = 1\ 363\ 794x$ for phosphate and $y = 2\ 654\ 272x - 2\ 719\ 126$ for ADP, where y corresponds to the absolute integral and x to the analyte concentration (mM). Concentrations in experimental samples were calculated by inserting the measured integral values into the corresponding equations. Spectra were recorded in D_2O using a Bruker spectrometer operating at 242.9 MHz for ^{31}P with proton decoupling (waltz16), a spectral width of 96153.844 Hz, 65 536 data points, and 16 scans. A relaxation delay (D1) of 2.0 s was used. Spectra were processed using exponential multiplication (LB = 1 Hz) and analyzed with MestReNova (version 14.2.0–26 256). ^{1}H NMR spectra were recorded on a Bruker Avance III spectrometer operating at 600 MHz. Samples were measured in an H_2O/D_2O mixture (6:1, v/v), with sodium 3-(trimethylsilyl)-1-propanesulfonate (DSS) as an internal chemical shift reference (methyl signal at 0.00 ppm). Spectra were acquired using a noesygppr1d pulse sequence with a relaxation delay (D1) of 1 s, a time-domain size of 98 520 points, and a spectral width of 12315.271 Hz. Sixteen scans were accumulated per sample. Additional acquisition parameters included an acquisition time of 4.0 s and water suppression via presaturation. Spectra were processed using exponential multiplication (LB = 0.3 Hz) and integrated using Chenomx NMR Suite (version 9.0).

Identification by ESI–LC–MS

The phosphorylated compounds cytidine 5-phosphate, phosphocreatine and ribose 5-phosphate were determined and quantified using the Dionex UltiMate 3000 UPLC system (Thermo Scientific, Germering, Germany) coupled to a maXis 4G (Bruker Daltonics, Bremen, Germany) quadrupole-time-of-flight (Q-TOF) mass spectrometer equipped with an electrospray (ESI) ion source. The separation was performed on a XSelect HSS T3 (100 Å, 2.5 µm, 3.0 × 150 mm; Waters, Milford, MA, USA) column at room temperature within a 20 min gradient at a flow rate of 0.3 $mL \cdot min^{-1}$ using a binary gradient system with water/0.1% formic acid (FA) as mobile phase A and methanol/0.1% FA as mobile phase B. The following gradient was used: 0 to 3 min 2% B (v/v), 3 to 10 min linear increase to 50% B, until 13 min linear increase to 95% B, hold at 95% B until 15 min, linear decrease to 2% B until 16 min, and finally, hold at 2% B until 20 min. The samples were diluted by a factor of 10; 10 µL of sample was injected. The ESI–LC–MS and ESI–LC–MS/MS analysis was performed using a Q-TOF MS (maXis 4G; Bruker Daltonics). The instrument was operated in negative-ion mode and the operating conditions were as follows: dry gas (nitrogen): 8.0 $L \cdot min^{-1}$, dry heater: 200 °C, nebulizer pressure: 1.0 bar, capillary voltage: 4500 V. Data acquisition was carried out under control of the Compass HyStar software (version 6.0) (Bruker, Bremen, Germany). The different phosphorylated compounds were quantified from full-scan MS data (mass range 50–6000 m/z) using the DataAnalysis (version 6.1) software (Bruker). The quantification is based on calibration curves obtained with commercially available standards. MS/MS spectra and the specific fragments for phosphorylated compounds in negative mode of m/z = 78.95 for PO_3^- and m/z = 96.97 for $H_2PO_4^-$ provided confirmation that it is a phosphorylated molecule.

Acknowledgements

We thank the Center for Molecular and Structural Analytics, Heinrich Heine University (CeMSA@HHU) for recording the NMR-spectroscopic data. We thank Maximilian Burmeister, Eleni Dafni, Max Brabender, Joseph Moran, and Mirko Basen for many helpful discussions and Dr. Katy Evans and Stefano Tenuta for discussions on Pd and platinum group metals in serpentinizing systems. We particularly thank Bernhard Schink for helpful suggestions and the proposal to investigate palladium as

© 2026 The Author(s). *The FEBS Journal* published by John Wiley & Sons Ltd on behalf of Federation of European Biochemical Societies.

a catalyst. This project has received funding from the European Research Council (ERC) under the European Union's Horizon 2020 research and innovation program (grant agreement no. 101018894). For funding, WFM thanks the ERC (101018894), WFM and HT thank the Deutsche Forschungsgemeinschaft (DFG) (MA1426/21-1/TU315/8-1) and the Volkswagen Foundation (Grant 96_742), HT thanks the Spanish Ministry of Science, Innovation and Universities for an ATRAE grant. Open Access funding enabled and organized by Projekt DEAL.

Conflict of interest

The authors declare no conflict of interest.

Author contributions

WFM, MLS, NKH, SM, JMP, and HT conceived and designed the study. MLS, NKH, SM, JMP, and HT carried out laboratory reactions and analytics. WFM, MLS, NKH, SM, JMP, and HT designed laboratory experiments and interpreted the data. All authors contributed to results discussion. WFM, MLS, and NKH drafted the manuscript. All authors edited the manuscript and approved the final version.

Peer review

The peer review history for this article is available at https://www.webofscience.com/api/gateway/wos/peer-review/10.1111/febs.70737.

Data availability statement

The data that support the findings of this study are available in Figs 1–6 and the Supporting Information of this article.

References

1 Westheimer FH (1987) Why nature chose phosphates. *Science* **235**, 1173–1178.
2 Schwartz AW (2006) Phosphorus in prebiotic chemistry. *Philos Trans R Soc B* **361**, 1743–1749.
3 Pasek MA (2008) Rethinking early earth phosphorus geochemistry. *Proc Natl Acad Sci USA* **105**, 853–858.
4 Joyce G (2002) The antiquity of RNA-based evolution. *Nature* **418**, 214–221.
5 Benner SA, Bell EA, Biondi E, Brasser R, Carell T, Kim HJ, Mojzsis SJ, Omran A, Pasek MA & Trail D (2020) When did life likely emerge on earth in an RNA-first process? *ChemSystemsChem* **2**, e1900035.
6 Eakin RE (1963) An approach to the evolution of metabolism. *Proc Natl Acad Sci* **49**, 360–366.
7 Fuchs G & Stupperich E (1985) Evolution of autotrophic CO_2 fixation. In Evolution of Prokaryotes (FEMS Symposium No. 29) (Schleifer KH & Stackebrandt E, eds). Academic Press, London.
8 Wächtershäuser G (1992) Groundworks for an evolutionary biochemistry: the iron-sulfur world. *Prog Biophys Mol Biol* **58**, 85–201.
9 Martin W & Russell MJ (2007) On the origin of biochemistry at an alkaline hydrothermal vent. *Philos Trans R Soc B Biol Sci* **362**, 1887–1926.
10 Lipmann F (1965) Projecting backward from the present stage of evolution of biosynthesis. In The Origin of Prebiological Systems and of their Molecular Matrices (Fox SW, ed.), pp. 259–280. Academic Press, New York.
11 Thauer RK, Jungermann K & Decker K (1997) Energy conservation in chemotrophic anaerobic bacteria. *Bacteriol Rev* **41**, 100–180.
12 Pasek MA, Gull M & Herschy B (2017) Phosphorylation on the early earth. *Chem Geol* **475**, 149–170.
13 Weller D, Matreux T, Smokers IBA, Schmid A, Mast CB, Dingwell DB, Braun D & Scheu B (2025) Magmatic immiscibility provides phosphate for prebiotic chemistry. *Sci Adv* **11**, eadz2567.
14 Wimmer JLE, Xavier JC, Vieira AN, Pereira DPH, Leidner J, Sousa FL, Kleinermanns K, Preiner M & Martin WF (2021) Energy at origins: favorable thermodynamics of biosynthetic reactions in the last universal common ancestor (LUCA). *Front Microbiol* **12**, 793664.
15 Mrnjavac N, Hoffmann NK, Schlikker ML, Burmeister M, Schwander L, García García C, Brabender M, Steel M, Huson DH, Metzger S *et al.* (2026) Intermediate stages in the origin of metabolism at a phosphorylating hydrothermal vent. *Sci Adv* **12**, eaef3128.
16 White AK & Metcalf WW (2007) Microbial metabolism of reduced phosphorus compounds. *Annu Rev Microbiol* **61**, 379–400.
17 Duhamel S (2025) The microbial phosphorus cycle in aquatic ecosystems. *Nat Rev Microbiol* **23**, 239–255.
18 Metcalf WW & Van Der Donk WA (2009) Biosynthesis of phosphonic and phosphinic acid natural products. *Annu Rev Biochem* **78**, 65–94.
19 Ramos-Figueroa JS, Palmer DRJ & Horsman GP (2022) Phosphoenolpyruvate mutase-catalyzed C–P bond formation: mechanistic ambiguities and opportunities. *Chembiochem* **23**, e202200285.
20 Pasek MA, Sampson JM & Atlas Z (2014) Redox chemistry in the phosphorus biogeochemical cycle. *Proc Natl Acad Sci USA* **111**, 15468–15473.
21 Toner JD & Catling DC (2020) A carbonate-rich lake solution to the phosphate problem of the origin of life. *Proc Natl Acad Sci USA* **117**, 883–888.

© 2026 The Author(s). *The FEBS Journal* published by John Wiley & Sons Ltd on behalf of Federation of European Biochemical Societies.

22 Lohrmann R & Orgel LE (1968) Prebiotic synthesis: phosphorylation in aqueous solution. *Science* **161**, 64–66.
23 Powner MW, Gerland B & Sutherland JD (2009) Synthesis of activated pyrimidine ribonucleotides in prebiotically plausible conditions. *Nature* **459**, 239–242.
24 Schoffstall AM (1976) Prebiotic phosphorylation of nucleosides in formamide. *Orig Life* **7**, 399–412.
25 Fernández-García C, Coggins AJ & Powner MW (2017) A chemist's perspective on the role of phosphorus at the origins of life. *Life* **7**, 31.
26 Zimmermann J, Mayer RJ & Moran J (2023) A single phosphorylation mechanism in early metabolism—the case of phosphoenolpyruvate. *Chem Sci* **14**, 14100–14108.
27 Gulick A (1955) Phosphorus as a factor in the origin of life. *Am Sci* **43**, 479–489.
28 Fuchs G (1986) CO_2 fixation in acetogenic bacteria: variations on a theme. *FEMS Microbiol Rev* **2**, 181–213.
29 Baross JA & Hoffman SE (1985) Submarine hydrothermal vents and associated gradient environments as sites for the origin and evolution of life. *Orig Life Evol Biosph* **15**, 327–345.
30 Martin W, Baross J, Kelley D & Russell MJ (2008) Hydrothermal vents and the origin of life. *Nat Rev Microbiol* **6**, 805–814.
31 Schink B & Friedrich M (2000) Phosphite oxidation by sulphate reduction. *Nature* **406**, 37.
32 Schink B, Thiemann V, Laue H & Friedrich MW (2002) *Desulfotignum phosphitoxidans* sp. nov., a new marine sulfate reducer that oxidizes phosphite to phosphate. *Arch Microbiol* **177**, 381–391.
33 Mao Z, Fleming JR, Mayans O, Frey J, Schleheck D, Schink B & Müller N (2023) AMP-dependent phosphite dehydrogenase, a phosphorylating enzyme in dissimilatory phosphite oxidation. *Proc Natl Acad Sci USA* **120**, e2309743120.
34 Buckel W (2001) Anorganische Chemie in Meeressedimenten. *Angew Chem* **113**, 1463–1464.
35 Herschy B, Chang SJ, Blake R, Lepland A, Abbott-Lyon H, Sampson J, Atlas Z, Kee TP & Pasek MA (2018) Archean phosphorus liberation induced by iron redox geochemistry. *Nat Commun* **9**, 1346.
36 Ewens SD, Gomberg AFS, Barnum TP, Borton MA, Carlson HK, Wrighton KC & Coates JD (2021) The diversity and evolution of microbial dissimilatory phosphite oxidation. *Proc Natl Acad Sci USA* **118**, e2020024118.
37 Pasek MA, Harnmeijer JP, Buick R, Gull M & Atlas Z (2013) Evidence for reactive reduced phosphorus species in the early Archean ocean. *Proc Natl Acad Sci USA* **110**, 10089–10094.
38 Frouin E, Lecoeuvre A, Armougom F, Schrenk MO & Erauso G (2022) Comparative metagenomics highlight a widespread pathway involved in catabolism of phosphonates in marine and terrestrial serpentinizing ecosystems. *mSystems* **7**, e0032822.
39 Schwander L, Brabender M, Mrnjavac N, Wimmer JLE, Preiner M & Martin WF (2023) Serpentinization as the source of energy, electrons, organics, catalysts, nutrients and pH gradients for the origin of LUCA and life. *Front Microbiol* **14**, 1257597.
40 Boden JS, Som SM, Brazelton WJ, Anderson RE & Stüeken EE (2025) Evaluating serpentinization as a source of phosphite to microbial communities in hydrothermal vents. *Geobiology* **23**, e70016.
41 Pasek MA, Omran A, Feng T, Gull M, Lang C, Abbatiello J, Garong L, Johnston R, Ryan J & Abbott-Lyon H (2022) Serpentinization as a route to liberating phosphorus on habitable worlds. *Geochim Cosmochim Acta* **336**, 332–340.
42 Lang SQ & Brazelton WJ (2020) Habitability of the marine serpentinite subsurface: a case study of the lost City hydrothermal field. *Philos Trans R Soc A Math Phys Eng Sci* **378**, 20180429.
43 Sleep NH, Bird DK & Pope EC (2011) Serpentinite and the dawn of life. *Philos Trans R Soc B* **366**, 2857–2869.
44 Bach W, Paulick H, Garrido CJ, Ildefonse B, Meurer WP & Humphris SE (2006) Unraveling the sequence of serpentinization reactions: petrography, mineral chemistry, and petrophysics of serpentinites from MAR 15° N (ODP leg 209, site 1274). *Geophys Res Lett* **33**, L13306.
45 Boyd ES, Amenabar MJ, Poudel S & Templeton AS (2020) Bioenergetic constraints on the origin of autotrophic metabolism. *Philos Trans A Math Phys Eng Sci* **378**, 20190151.
46 Chamberlain JA, McLeod CR, Traill RJ & Lachance GR (1965) Native metals in the muskox intrusion. *Can J Earth Sci* **2**, 188–215.
47 Preiner M, Igarashi K, Muchowska KB, Yu M, Varma SJ, Kleinermanns K, Nobu MK, Kamagata Y, Tüysüz H, Moran J *et al.* (2020) A hydrogen dependent geochemical analogue of primordial carbon and energy metabolism. *Nat Ecol Evol* **4**, 534–542.
48 Beyazay T, Ochoa-Hernández C, Song Y, Belthle KS, Martin WF & Tüysüz H (2023) Influence of composition of nickel-iron nanoparticles for abiotic CO_2 conversion to early prebiotic organics. *Angew Chem Int Ed* **62**, e202218189.
49 Song Y, Beyazay T & Tüysüz H (2024) Effect of alkali- and alkaline-earth-metal promoters on silica-supported Co–Fe alloy for autocatalytic CO_2 fixation. *Angew Chem* **136**, e202316110.
50 Kaur H, Rauscher SA, Werner E, Song Y, Yi J, Kazöne W, Martin WF, Tüysüz H & Moran J (2024) A prebiotic Krebs cycle analog generates amino acids with H_2 and NH_3 over nickel. *Chem* **10**, 1528–1540.

© 2026 The Author(s). *The FEBS Journal* published by John Wiley & Sons Ltd on behalf of Federation of European Biochemical Societies.

51 Schlikker ML, Brabender M, Schwander L, Garcia Garcia C, Burmeister M, Metzger S, Moran J & Martin WF (2024) Conversion of pyridoxal to pyridoxamine with NH_3 and H_2 on nickel generates a protometabolic nitrogen shuttle under serpentinizing conditions. *FEBS J* **292**, 3041–3055.

52 He D, Wang X, Yang Y, He R, Zhong H, Wang Y, Han B & Jin F (2021) Hydrothermal synthesis of long-chain hydrocarbons up to C_{24} with $NaHCO_3$-assisted stabilizing cobalt. *Proc Natl Acad Sci USA* **118**, e2115059118.

53 Henriques Pereira DP, Leethaus J, Beyazay T, do Nascimento Vieira A, Kleinermanns K, Tüysüz H, Martin WF & Preiner M (2022) Role of geochemical protoenzymes (geozymes) in primordial metabolism: specific abiotic hydride transfer by metals to the biological redox cofactor NAD^+. *FEBS J* **289**, 3148–3162.

54 Henriques Pereira DP, Xie X, Stewart SV, Subrati Z, Beyazay T, Paczia N, Belz J, Volz K, Erastova V, Tüysüz H *et al.* (2025) Reduction of NAD and NMN on mineral surfaces with H_2 reveals a functional role for the AMP moiety in a prebiotic context. *Commun Chem* **8**, 318.

55 Brabender M, Henriques Pereira DP, Mrnjavac N, Schlikker ML, Kimura ZI, Sucharitakul J, Kleinermanns K, Tüysüz H, Buckel W, Preiner M *et al.* (2024) Ferredoxin reduction by hydrogen with iron functions as an evolutionary precursor of flavin-based electron bifurcation. *Proc Natl Acad Sci USA* **121**, e2318969121.

56 Martin WF, Hoffmann NK & Schlikker ML (2026) Shiny metal catalysts at the origin of metabolism. *Trends Microbiol*. in press. doi: 10.1016/j.tim.2026.07.012

57 Lawley CJM, Petts DC, Jackson SE, Zagorevski A, Pearson DG, Kjarsgaard BA, Savard D & Tschirhart V (2020) Precious metal mobility during serpentinization and breakdown of base metal sulphide. *Lithos* **354–355**, 105278.

58 Kutyrev A, Kamenetsky VS, Kontonikas-Charos A, Savelyev D & Yakich T (2023) Behavior of platinum-group elements during hydrous metamorphism: constraints from awaruite (Ni_3Fe) mineralization. *Lithosphere* **2023** , 126.

59 Evans K, Reddy SM, Merle R, Fougerouse D, Rickard WDA, Saxey DW, Park JW, Doucet L & Jourdan F (2023) The origin of platinum group minerals in oceanic crust. *Geology* **51**, 554–558.

60 Yang K & Metcalf WW (2004) A new activity for an old enzyme: *Escherichia coli* bacterial alkaline phosphatase is a phosphite-dependent hydrogenase. *Proc Natl Acad Sci USA* **101**, 7919–7924.

61 Modjewski LD, Johnsen U, Schönheit P & Martin WF (2025) The early evolution of the glycolytic pathway from autotrophic origins to glycogen and back. *FEMS Microbiol Rev* **49**, fuaf049.

62 Keller MA, Turchyn AV & Ralser M (2014) Non-enzymatic glycolysis and pentose phosphate pathway–like reactions in a plausible Archean ocean. *Mol Syst Biol* **10**, MSB145228.

63 Mrnjavac N, Wimmer JLE, Brabender M, Schwander L & Martin WF (2023) The moon-forming impact and the autotrophic origin of life. *ChemPlusChem* **88**, e202300270.

64 Sleep NH, Meibom A, Fridriksson T, Coleman RG & Bird DK (2004) H_2-rich fluids from serpentinization: geochemical and biotic implications. *Proc Natl Acad Sci USA* **101**, 12818–12823.

65 Arndt NT & Nisbet EG (2012) Processes on the young earth and the habitats of early life. *Annu Rev Earth Planet Sci* **40**, 521–549.

66 Tamblyn R & Hermann J (2023) Geological evidence for high H_2 production from komatiites in the Archaean. *Nat Geosci* **16**, 1194–1199.

67 Halmann M, Sanchez RA & Orgel LE (1969) Phosphorylation of D-ribose in aqueous solution. *J Org Chem* **34**, 3702–3703.

68 Degani C & Halmann M (1971) D-glucose 1-phosphate formation by cyanogen-induced phosphorylation of D-glucose: synthesis, mechanism, and application to other reducing sugars. *J Chem Soc* 1459–1465.

69 Lowry OH, Carter J, Ward JB & Glaser L (1971) The effect of carbon and nitrogen sources on the level of metabolic intermediates in *Escherichia coli*. *J Biol Chem* **246**, 6511–6521.

70 Sojo V, Pomiankowski A & Lane N (2014) A bioenergetic basis for membrane divergence in archaea and bacteria. *PLoS Biol* **12**, e1001926.

71 Pasek MA, Dworkin JP & Lauretta DS (2007) A radical pathway for organic phosphorylation during schreibersite corrosion with implications for the origin of life. *Geochim Cosmochim Acta* **71**, 1721–1736.

72 Wald G (1964) The origins of life. *Proc Natl Acad Sci USA* **52**, 595–611.

73 Berg JM, Tymoczko JL, Gatto GJ Jr & Stryer L (2015) Biochemistry. 8th edn. Macmillan, New York, NY.

74 Buckel W & Eggerer H (1965) On the optical determination of citrate synthase and acetyl-coenzyme a. *Biochem Z* **343**, 29–43.

75 Gibard C, Gorrell IB, Jiménez EI, Kee TP, Pasek MA & Krishnamurthy R (2019) Geochemical sources and availability of amidophosphates on the early earth. *Angew Chem Int Ed* **58**, 8151–8155.

76 Müller V, Chowdhury NP & Basen M (2018) Electron bifurcation: a long-hidden energy-coupling mechanism. *Annu Rev Microbiol* **72**, 331–353.

77 Mitchell P (1961) Coupling of phosphorylation to electron and hydrogen transfer by a chemi-osmotic type of mechanism. *Nature* **191**, 144–148.

© 2026 The Author(s). *The FEBS Journal* published by John Wiley & Sons Ltd on behalf of Federation of European Biochemical Societies.

78 Gaudet G, Forano E, Dauphin G & Delort AM (1992) Futile cycling of glycogen in *Fibrobacter succinogenes* as shown by in situ ^{1}H-NMR and ^{13}C-NMR investigation. *Eur J Biochem* **207**, 155–162.
79 Kornberg A (1962) On the metabolic significance of phosphorolytic and pyrophosphorolytic reactions. In Horizons in Biochemistry (Kasha H & Pullman B, eds), pp. 251–264. Academic Press, New York.
80 Wimmer JLE, Kleinermanns K & Martin WF (2021) Pyrophosphate and irreversibility in evolution, or why PPi is not an energy currency and why nature chose triphosphates. *Front Microbiol* **12**, 759359.
81 Kornberg A, Rao NN & Ault-Riche D (1999) Inorganic polyphosphate: a molecule of many functions. *Annu Rev Biochem* **68**, 89–125.
82 Höfmann S, Kogay R, Schmerling C, Stracke C, Niemeyer F, Schaller T, Makarova KS, Koonin EV, Snoep JL, Bräsen C *et al.* (2026) Identification of a distinct family of polyphosphate kinases relevant to energy homeostasis in Crenarchaeota. *J Biol Chem* **302**, 4.
83 Gull M, Centlivre J, Feng T, Smith B, Johnson-Finn KN, Rogers KL, McCallum SA & Pasek MA (2025) Implausibility of hypophosphate on the early earth and today. *Discov Chem* **2**, 259.
84 Gan D, Ying J & Zhao Y (2022) Prebiotic chemistry: the role of trimetaphosphate in prebiotic chemical evolution. *Front Chem* **10**, 941228.
85 Relyea HA & van der Donk WA (2005) Mechanism and applications of phosphite dehydrogenase. *Bioorg Chem* **33**, 171–189.
86 Di Sabato G & Jencks WP (1961) Mechanism and catalysis of reactions of acyl phosphates. II. Hydrolysis. *J Am Chem Soc* **83**, 4393–4400.
87 Cleland WW & Hengge AC (2006) Enzymatic mechanisms of phosphate and sulfate transfer. *Chem Rev* **106**, 3252–3278.
88 Choe JY, Iancu CV, Fromm HJ & Honzatko RB (2003) Metaphosphate in the active site of fructose-1,6-bisphosphatase. *J Biol Chem* **278**, 16015–16020.
89 Krachtus D, Smith JC & Imhof P (2018) Quantum mechanical/molecular mechanical analysis of the catalytic mechanism of phosphoserine phosphatase. *Molecules* **23**, 3342.
90 Brás NF, Fernandes PA, Ramos MJ & Schwartz SD (2018) Mechanistic insights on human phosphoglucomutase revealed by transition path sampling and molecular dynamics calculations. *Chem A Eur J* **24**, 1978–1987.
91 Westheimer FH (1981) Monomeric metaphosphates. *Chem Rev* **81**, 313–326.
92 Schwartz AW (1997) Prebiotic phosphorus chemistry reconsidered. *Orig Life Evol Biosph* **27**, 505–512.
93 Gull M, Cruz HA, Krishnamurthy R & Pasek MA (2025) Phosphorylation of nucleosides by PN bond species generated from prebiotic reduced phosphorus sources. *Commun Chem* **8**, 187.
94 Gull M, Feng T, Cruz HA, Krishnamurthy R & Pasek MA (2023) Prebiotic chemistry of phosphite: mild thermal routes to form condensed-P energy currency molecules leading up to the formation of organophosphorus compounds. *Life* **13**, 920.
95 Whicher A, Camprubi E, Pinna S, Herschy B & Lane N (2018) Acetyl phosphate as a primordial energy currency at the origin of life. *Orig Life Evol Biosph* **48**, 159–179.
96 Toland WG & Campbell RW (1963) Thiolesters by anhydride reduction with hydrogen sulfide. *J Org Chem* **28**, 3124–3129.
97 Chen W, Zimmermann J, Dechent J & Moran J (2025) Nonenzymatic carboxylate phosphorylation in water. *Eur J Org Chem* **28**.
98 Osumah A & Krishnamurthy R (2021) Diamidophosphate (DAP): a plausible prebiotic phosphorylating reagent with a chem to BioChem potential? *Chembiochem* **22**, 3001–3009.
99 Meyerhof O, Shatas R & Kaplan A (1953) Heat of hydrolysis of trimetaphosphate. *Biochim Biophys Acta* **12**, 121–127.
100 Weiss MC, Sousa FL, Mrnjavac N, Neukirchen S, Roettger M, Nelson-Sathi S & Martin WF (2016) The physiology and habitat of the last universal common ancestor. *Nat Microbiol* **1**, 16116.
101 Nagaosa Y & Aoyama E (2001) Catalytic oxidation of phosphite and hypophosphite to phosphate on Pd/activated carbon powder. *Carbon* **39**, 2087–2088.
102 Huwiler SG, Löffler C, Anselmann SEL, Stärk HJ, von Bergen M, Flechsler J, Rachel R & Boll M (2019) One-megadalton metalloenzyme complex in *Geobacter metallireducens* involved in benzene ring reduction beyond the biological redox window. *Proc Natl Acad Sci USA* **116**, 2259–2264.
103 de Duve C (1998) Clues from present-day biology: the thioester world. In The Molecular Origins of Life (Brack A, ed.), pp. 219–236. Cambridge University Press, Cambridge, MA.
104 Sanden SA, Butch C, Bartlett S, Virgo N, Sekine Y & McGlynn S (2025) Rapid hydrolysis rates of thio- and phosphate esters constrain the origin of metabolism to cool, acidic to neutral environments. *iScience* **28**, 106889.
105 Goldford JE, Hartman H, Marsland R III & Segrè D (2019) Environmental boundary conditions for the origin of life converge to an organo-sulfur metabolism. *Nat Ecol Evol* **3**, 1715–1724.
106 Goldford JE, Hartman H, Smith TF & Segrè D (2017) Remnants of an ancient metabolism without phosphate. *Cell* **168**, 1126–1134.
107 Patel BH, Percivalle C, Ritson DJ, Duffy CD & Sutherland JD (2015) Common origins of RNA,

© 2026 The Author(s). *The FEBS Journal* published by John Wiley & Sons Ltd on behalf of Federation of European Biochemical Societies.

protein and lipid precursors in a cyanosulfidic protometabolism. *Nat Chem* **7**, 301–307.
108 Russell MJ, Hall AJ & Martin W (2010) Serpentinization as a source of energy at the origin of life. *Geobiology* **8**, 355–371.
109 Lane N, Allen JF & Martin W (2010) How did LUCA make a living? Chemiosmosis in the origin of life. *Bioessays* **32**, 271–280.
110 Yu F, Fei J, Jia Y, Wang T, Martin WF & Li J (2025) Chemiosmotic ATP synthesis by minimal protocells. *Cell Rep Phys Sci* **6**, 102461.
111 Herrmann G, Jayamani E, Mai G & Buckel W (2008) Energy conservation via electron-transferring flavoprotein in anaerobic bacteria. *J Bacteriol* **190**, 784–791.

Supporting information

Additional supporting information may be found online in the Supporting Information section at the end of the article.

Fig. S1. Raw ^{31}P and ^{1}H NMR data for ADP formation under phosphite-driven phosphorylation conditions.
Fig. S2. ^{1}H NMR and ESI–LC–MS data supporting cytidine formation under phosphite-driven phosphorylation conditions.
Fig. S3. ^{1}H NMR and ESI–LC–MS data supporting ribose transformation under phosphite-driven phosphorylation conditions.
Fig. S4. NMR data supporting glucose phosphorylation under phosphite-driven conditions.
Fig. S5. Formation of glycerol phosphate monitored by ^{31}P and ^{1}H NMR under phosphite-driven phosphorylation conditions.
Fig. S6. ^{31}P and ^{1}H NMR spectra of serine phosphorylation under phosphite-driven conditions with Pd/C.
Fig. S7. ^{31}P and ^{1}H NMR spectra of serine phosphorylation under phosphite-driven conditions with Pd^{0}.
Fig. S8. ^{31}P and ^{1}H NMR spectra of acetate–-phosphite–Pd/C suspensions under phosphite-driven conditions.
Fig. S9. NMR and ESI–LC–MS data supporting phosphocreatine formation under phosphite-driven conditions.
Fig. S10. Phosphite oxidation to phosphate under hydrogen atmosphere.
Fig. S11. Structural characterization of Pd-awaurite.
Fig. S12. ADP formation under H2-driven phosphorylation conditions.
Table S1. Raw NMR spectral data and corresponding product yields (mM).
Table S2. Raw ESI-LC–MS data and corresponding calculated product yields obtained from reactions containing Phi (200 mM) and ribose, cytidine, and creatine (100 mM each).
Table S3. Raw ESI-LC–MS data and calculated product yields obtained from reactions containing AMP (100 mM) and Phi (200 mM).

© 2026 The Author(s). *The FEBS Journal* published by John Wiley & Sons Ltd on behalf of Federation of European Biochemical Societies.